

Jennifer M. Cram^{1*}, Yubao Liu¹, Simon Low-Nam¹,
 Rong-Shyang Sheu¹, Laurie Carson, Christopher A. Davis¹, Tom Warner¹, James F. Bowers²
¹NCAR/RAP, Boulder, Colorado

² U.S. Army Dugway Proving Ground, West Desert Test Center, Dugway, Utah

1. INTRODUCTION

A mesoscale, real-time, four-dimensional data assimilation (RT-FDDA) and short-term forecasting system has been developed for the U.S. Army Test and Evaluation Command (ATEC) at Dugway Proving Ground (DPG) in Utah. The DPG RT-FDDA system, which has been operational since the summer of 2000, is designed around the Pennsylvania State University/National Center for Atmospheric Research (PSU/NCAR) MM5 model. It uses a cycling methodology which provides the end-user with a continuous series of updated 3-dimensional analyses and a new 12-hr forecast on 3 domains (30 km, 10km, and 3.3 km grid spacings) every 3 h in real-time. The multi-stage cycling methodology is designed to take best advantage of the differing data ingest lags encountered in a real-time system (valid time lags can range from only a few minutes to 2 h), and uses a model-restart capability to provide continuous, balanced, 3-dimensional analyses and forecasts at any time interval. The FDDA system is a continuous assimilation system (Newtonian relaxation), and uses many diverse data sets, with availability frequencies ranging from 10 minutes to 12 h: standard surface and upper air observations, special surface observations, the University of Utah Mesowest observations (extensive western U.S. mesonet), DPG local surface observations, DPG profilers and RASS instrumentation, and NESDIS GOES wind vectors. The RT-FDDA system will be described, from design to product availability to computational performance, and performance results will be presented.

2. ASSIMILATION CONCEPTS

The concept of dynamically combining observational and model data, i.e. the concept of Four-Dimensional Data Assimilation (FDDA) was introduced by Charney et al. (1969). FDDA concepts and applications since then can mostly be classified in two areas; intermittent and continuous schemes.

Intermittent FDDA uses some sort of analysis scheme (successive correction, OI, 3D-VAR) to combine a first-guess field with observations. The new analysis is then used to initialize a model which is integrated forward; that forecast may be the new first-guess for the next analysis. The analysis time intervals for such schemes typically range from 1 hr to 12 hrs. Disadvantages of such schemes, especially on the mesoscale, include analysis balance constraints, model spin-up, data sparseness, and data usage constraints. Many analyses apply balance constraints either explicitly or implicitly through multivariate schemes;

Corresponding author address: Jennifer M. Cram, NCAR/RAP, P.O. Box 3000, Boulder, CO 80307-3000; email: cram@ucar.edu

such balances (geostrophic thermal wind, etc.) are usually appropriate only at synoptic scales. Cloud and moisture processes may require several hours of spin-up time from initialization. In data-sparse areas an analysis may be only as good as its first-guess; if that first guess is from a synoptic scale model the circulations will not reflect mesoscale features. Finally, observational data in intermittent assimilation schemes can only be used at the intermittent analysis times. Many surface mesonets and observation types (profiler, RASS) have observation frequencies on the scale of 5-20 mins, and even standard WMO surface observation data sets include off-hour special observations.

Continuous assimilation schemes have the ability to assimilate observational data at its valid time, and produce smoothly varying model fields in all 4 dimensions. The time-continuous aspect of such schemes can eliminate the model spin-up problem, and allows for the usage of all available observations. Such schemes are more appropriate for observations on both time and space mesoscales because the model adjusts dynamically; inappropriate larger scale balances are not imposed. Examples of continuous assimilation methodologies include 4-Dimensional Variational (4DVAR) methods and Newtonian relaxation of observations (obs nudging). The former is not computationally feasible for real-time or operational assimilation systems. The Newtonian relaxation technique is described well in Stauffer and Seaman (1990), including the differences between analysis nudging and obs nudging. Analysis nudging is often considered to be a continuous assimilation method because the analyses are nudged into the model continuously over time. However, the analysis itself is a one-time product and thus analysis nudging has many of the disadvantages associated with intermittent assimilation schemes, including data sparseness and balance issues. One of the main disadvantages of obs nudging schemes is that the observations must be of a model variable, or directly convertible to one. Indirect observations, such as satellite-measured radiances, cannot be assimilated via obs nudging.

Recent studies using Newtonian relaxation include those of Stauffer and Seaman (1994), Stauffer et al. (1991), Seaman et al. (1995), and Fast (1995). A common finding of these studies has been that analysis nudging works well (better than intermittent assimilation) on synoptic scales, where observation frequencies are on the order of 3-12 hours, almost all observations are clustered around those times, and the synoptic scale analysis is deemed accurate and representative of the circulations of interest. Stauffer and Seaman (1994) and Seaman et al. (1995) found that obs nudging was more successful on the mesoscale. Leslie et al. (1998) found that the impact of obs nudging was similar to the impact of assimilating

the same data in a 4DVAR system, noting that the former was practicable while the latter was too computationally expensive.

3. RT-FDDA SYSTEM DESIGN

The NCAR/RAP ATEC MM5-based RT-FDDA system is designed to run in real-time, providing both analyses and short-term forecasts. The data assimilation method (Newtonian relaxation) allows for a time-continuous system and use of observational data at all times (not just on-the-hour). Each new model cycle is a restart from the previous final FDDA cycle analyses; no extra time is needed for cloud or precipitation spin-up.

The RT-FDDA system uses a 3-hr cycling method, with three separate stages within each 3-hr cycle. Every 3 hours in real time (starting at 0200 UTC, 0500 UTC, 0800 UTC, etc.) the system completes 3 simulation hours of "final" FDDA analysis, 3 simulation hours of "preliminary" FDDA analysis, and then 6-12 simulation hours of pure forecast. Two data assimilation stages (preliminary and final, with different data cutoff windows) are used in order to incorporate all possible data. On all three grids new updated analyses (preliminary and final) and a new 6-12 hr forecast are produced every 3 hours real-time. Fig. 1 illustrates the cycle/stage design of the RT-FDDA system.

The final FDDA stage uses continuous observation nudging on all three model grids and runs 2-4 hours behind real time, allowing time for data ingest lags. The final stage simulation is initialized as a restart from the previous cycle's final stage simulation; it is a continuation of the previous cycle's final simulation and thus does not require any spin-up for diabatic or dynamic processes. Over time, the final stages in each cycle link together and form one long continuous simulation. The preliminary FDDA stage is a restart from the final stage and thus a continuous model run, again without diabatic or dynamic spin-up problems. The preliminary stage uses whatever data is available within its integration window (from approximately 2 hrs previous up to the current time). This stage will miss late observations and some lagged data sets, but usually incorporates most of the surface observation data sets. The short-term forecast stage restarts/continues from the preliminary cycle results. By the time this stage starts the model simulation time has passed the current real time and no more observations are available.

4. MODEL CONFIGURATION AND SPECIFICS

The PSU/NCAR MM5 Version 4 (Grell et al., 1995) is used as the basis of this modeling system.

4.1 Domain configuration

The RT-FDDA system designed for ATEC's Dugway Proving Ground (DPG) runs in a 3-grid configuration centered over Utah, as shown in Fig. 2. All domains have 31 layers in the vertical, with the model top at 50 hPa.

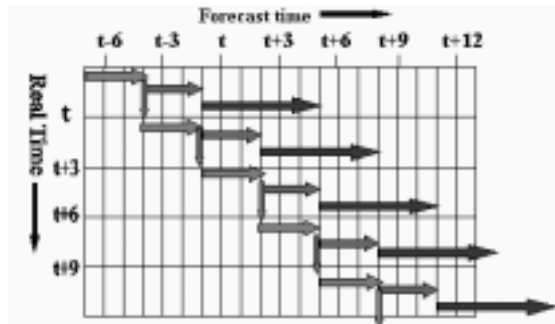


Fig. 1. Cycle diagram for the RT-FDDA system. Every 3 hours,: a) (lightest gray) final nudging stage, from $t-4$ to $t-1$. This stage is initialized as a re-start from the previous cycle's final stage; b) (medium gray) preliminary FDDA nudging stage from $t-1$ to $t+2$, restarts from final cycle analysis at $t-1$; c) (darkest gray) forecast from $t+2$ onwards.

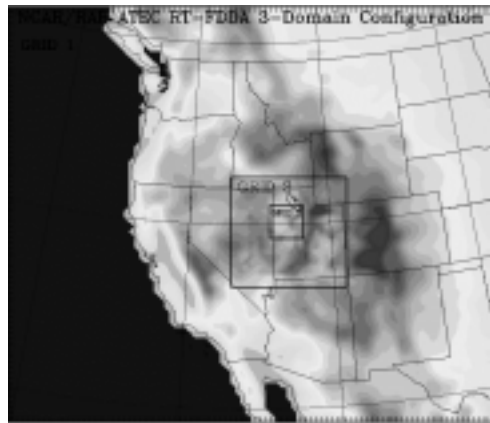


Fig. 2. The 3-domain configuration used for the NCAR/RAP ATEC RT-FDDA system. Grid 1 has a 30 km horizontal spacing with 96×84 grid points. Grid 2 has a 10 km spacing with 70×67 grid points. Grid 3 has a 3.3 km spacing with 61×61 grid points.

4.2 MM5 Configuration

The basic MM5 model configuration used in the RT-FDDA system is summarized as:

- Non-hydrostatic
- Interactive nesting procedure
- Radiative top boundary condition
- Time-changing lateral boundary conditions
- Grell cumulus parameterization on 10+ km grids.
- Simple ice explicit moisture scheme
- MRF (or Hong-Pan) PBL scheme
- Cloud radiation scheme
- Multi-layer soil temperature model
- Simple soil moisture variability bucket scheme
- Snow fall/melt scheme (Low-Nam et al., 2001)

4.3 Newtonian Relaxation algorithm

Newtonian Relaxation (nudging) of observations (vs. analysis nudging) is used to assimilate the observations into the MM5 model. The FDDA Newtonian relaxation algorithm as implemented in the

MM5 model is documented in Grell et al. (1995). Although many of the concepts and algorithms from the standard MM5 nudging software were retained, the observation nudging routines were substantially re-written for this RT-FDDA system and some of the concepts only available to the analysis nudging routines in the standard MM5 release were adapted to apply to the observation nudging routines. The nudging factor is set to $6.E-4s^{-1}$ for all variables (u,v,T,q) and is equivalent to a forcing time scale of approximately 30 minutes. The maximum horizontal radius varies with domain: R=240 km on grid 1, 120 km on grid 2, and 80 km on grid 3. The time window is +/- 40 minutes around the observation's valid time.

For surface observations there is an additional factor related to the difference between the surface pressure at the observation point and the surface pressure of an ij column; this factor reduces the effect of observations that are close horizontally but at different elevations. The surface observations are also adjusted to the model's lowest sigma level via a "reverse similarity theory" factor. Finally, the surface observation increment is also weighted upwards within the pbl. The vertical weighting algorithm for upper air observations is again similar to that described in Grell et al. (1995). A difference is that observations are not pre-interpolated to the model sigma levels and single-level upper air observations (such as satellite wind observations) can be assimilated.

4.4 Lateral Boundary Conditions

The lateral boundary condition algorithm used inside the MM5 model is the standard nudging towards the time-dependent externally-specified (ETA model) tendencies. Because of the real-time aspect of the RT-FDDA system, as well as the ongoing long-term forecast aspect (final stage forecasts from restarts can easily go for 10 days), special techniques were required for deriving the lateral boundary condition tendencies.

For each RT-FDDA cycle, the sequence of latest available ETA forecast 3-hr tendencies are used, with an anchoring of each new eta tendency back to the tendency used previously in the RT-FDDA system. The anchoring/differencing is necessary in order to eliminate systematic ETA errors that accumulate and become significant at the RT-FDDA lateral boundaries. Such areas can have geographic causes (always occur in the lee of a certain mountain range) or be related to specific synoptic situations. Without the anchoring those biases accumulate over several days in the RT-FDDA system and become significant.

4.5 System cold-start

A cold-start to the RT-FDDA system is when it starts from scratch from an ETA analysis (no restart from previous final stage output). This can be done at regular intervals, or as forced by some system problem. A cold-start is conceptually also a necessity at some regular interval to bring the model atmosphere back into line with reality - it could diverge from the real atmosphere despite the ETA lateral boundary condition

Obs totals	Grid 1	Grid 2	Grid 3
Metars	441	42	6
Specials	19	0	0
Ship	36	0	0
U of Utah	2870	827	257
Raob T,Td	30	3	1
Raob Wnd	29	3	1
Sat-wind	0	0	0
SAMS	95	95	95
Profiler	0	0	0

Table 1: Obs totals for +/-40 mins around 2001042600.

forcing and the final stage observation nudging. It is unclear at this point what this time limit is; we generally force a cold-start approximately every 7 days.

4.6 Data sets and Quality Control

The continuous assimilation method allows the use of observations at all times, not just those clustered around the 12-hourly, 3-hourly, or even hourly times. The University of Utah coordinates the compilation of observations from close to 20 different networks in the western US, many with observation frequencies of 15 minutes or less (Horel et al., 2000) , and all of those observations are incorporated into this system, along with standard WMO observations (surface, upper air, and asynoptic specials). Also, since this system was developed for an ATEC range there is a local automated surface mesonet on the range with observations at 15 min periods, and local profilers and RASS instrumentation with observations available at 20 min intervals. Satellite-derived wind information available from NESDIS (Gray et al., 1996; Nieman et al., 1997) is also incorporated into the system (sensitivity tests with this data set in the RT-FDDA system are described in Cram et al., 2001). Table 1 shows the typical surface data availability within +/- 40 minutes around the top of the hour on all 3 grids.

The quality control software performs gross error checks, buddy checks, and checks against a first-guess as defined by the previous cycle's preliminary and forecast stages. The WMO data sets, Utah Mesonet data sets, NESDIS satellite winds, and ATEC range surface mesonet data sets are processed with this quality control. The ATEC range profiler and RASS data sets have their own quality control thresholds.

5. COMPUTATIONAL HARDWARE

The NCAR/RAP ATEC RT-FDDA system has been run successfully on both shared and distributed memory platforms. The shared memory system runs on an 8-processor SGI O2000 in real time with a 6-hr forecast stage and the distributed memory system runs on an 8-node (16 processor) linux cluster with gigabit ethernet networking, with a 12-hr forecast stage.

6. WWW-BASED OUTPUT

The model output from the RT-FDDA system is processed as it is produced by the system. The model output time frequency for this system is hourly, although it can be increased or decreased as needed. At each

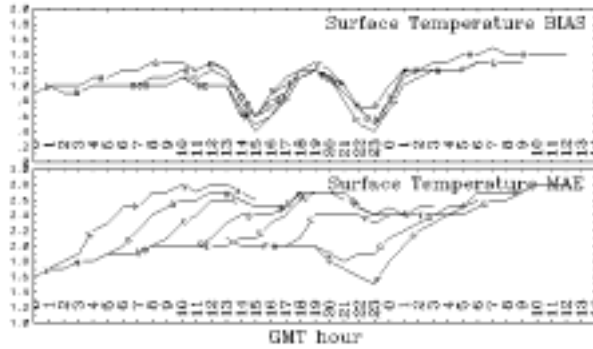


Fig. 3. Cycle-dependent surface temperature bias (deg C, top) and MAE (deg C, bottom) curves for the period from 2001010100 through 2001031500 for all 3 domains. The 8 consecutive lines (A, B, C, ...H) correspond to the statistics for the 8 daily cycles (the 0200, 0500, 0800, ... 2300 UTC cycles). The line for each cycle extends across all valid times (3 final hours, 3 prelim hours, 12 forecast hours), and the horizontal axis is the valid time. For example, the 0500 UTC cycle line (B) extends from 0200 UTC through 1900 UTC (0200-0400 UTC are final, 0500-0700 UTC are preliminary, 0800-1900 UTC are the forecast).

output time plots are generated of horizontal fields, vertical cross-sections, soundings, and observational data sets on all 3 grids. These images are then moved to a web-server with a GUI display tool.

7. RESULTS AND DISCUSSION

Statistics on the RT-FDDA system performance have been calculated since fall of 2000 for both surface and upper air observations. For surface observations the model variable is interpolated to the observation location and a temperature adjustment dependent on the difference between the model elevation and the observation elevation is added in. For upper air observations the model variables are interpolated both horizontally and to the standard pressure levels.

7.1 Cycle-dependent Surface statistics

The cycle-dependent average surface temperature bias and mean absolute error (MAE), on all 3 domains, for the time period from 2001010100 through 2001031512 are shown in Fig. 3. In each figure the 8 consecutive lines (A, B, C, ...H) correspond to the statistics for the 8 daily cycles (the 0200, 0005, 0800, ... 2300 UTC cycles). The line for each cycle extends across all valid times in the cycle (3 final hours, 3 prelim hours, 12 forecast hours), and the horizontal axis is the valid time. The bias set of curves is especially interesting as it shows a very consistent model dependence on valid time. The model biases are consistently lowest in the 1400-1600 UTC and 2200-0000 UTC time periods (the day/night transition times), irregardless of whether the cycle is in the final, prelim, or forecast stage. In contrast to the temperature bias curve the mixing ratio and wind speed biases (not shown) have only 1 minimum in the 1800-2200 UTC period. The MAE curve in Fig. 3 gives a nice view of the

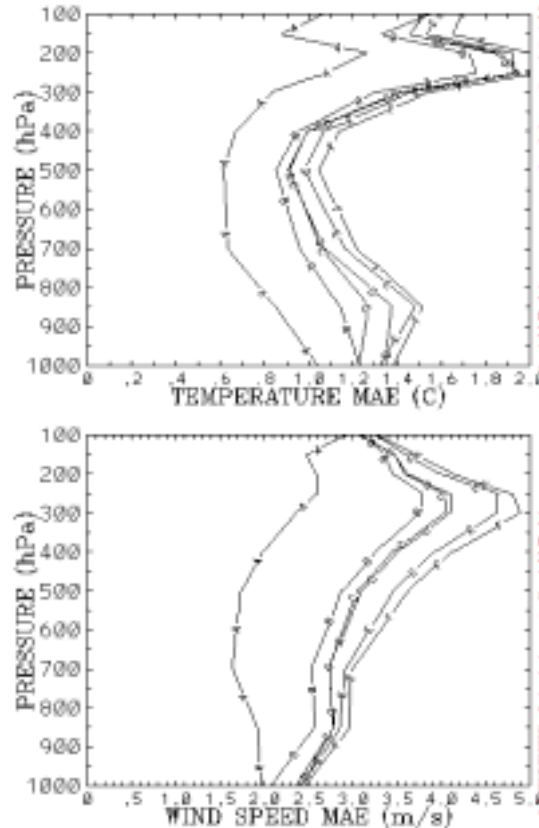


Fig. 4. The stage-dependent average upper air MAE for the time period from 2001010100 through 2001031512 on all 3 domains for temperature and wind speed. Each vertical curve is the level-dependent MAE for a particular stage, calculated at all valid synoptic times within the period. Curve A is for the final cycles that are valid at 0000 and 1200 UTC (from the 0200 and 1400 UTC cycles), curve B is for the preliminary cycles valid at the same synoptic times (from the 2300 and 1100 UTC cycles), curve C is the 2-hr forecast (2000 and 0800 UTC cycles), curve D is the 5-hr forecast (1700 and 0500 UTC cycles), curve E is the 8-hr forecast (1400 and 0200 UTC cycles), and curve F is the 11-hr forecasts (1100 and 2300 UTC cycles).

assimilation vs. forecast aspects of the cycles. The bottom of the curve envelope is the curve of the continuous final parts of the cycles – each consecutive final cycle restarts from the previous final cycle. Within each cycle the preliminary and then forecast stages diverge upwards from that lowest error final curve.

7.2 Stage-dependent upper air statistics

The stage-dependent average upper air MAE statistics for the time period from 2001010100 through 2001031512 and all 3 domains are shown in Fig. 4 for temperature and wind speed. In these graphs each vertical curve is the level-dependent MAE for a particular stage, with the statistics calculated at all valid synoptic times within the period. As would be expected the MAE decreases with the time distance from the final stage – increasing forecast lengths have higher MAEs and the preliminary stage MAE is greater than the final stage MAE.

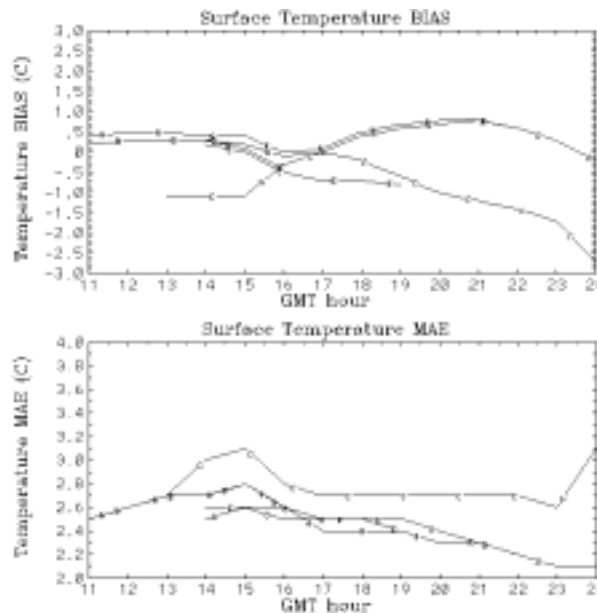


Fig. 5. Comparison of surface temperature MAE as a function of valid time (GMT hour) for forecasts from the RT-FDDA system and forecasts from a traditional analysis/forecast system. Both systems have the same grid configuration, with statistics calculated over domain 2. Curve A in is for the forecast from the 0800 UTC RT-FDDA cycle (0500-0700 UTC final, 0800-1000 UTC preliminary, then 1100-2200 UTC forecast). Curve B is the same as Curve A but for a 6 hr forecast from a parallel RT-FDDA system with a simple soil moisture and snow scheme, Curve C is the traditional forecast initialized at 1200 UTC (1300 through 0000 UTC for first 12 hrs), Curve D is the same as curve A except for the cycle 3 hrs later, and curve E is the same as curve B except for the cycle 3 hrs later.

7.3 RT-FDDA vs. standard forecast statistics

One of the expectations of this RT-FDDA system is that the continuous assimilation methodology will result in both decreased error and more consistently balanced (appropriate to the mesoscale) model fields on all grids, and then better forecasts from these grids. One way to measure whether the RT-FDDA system can provide better forecasts is to compare to a traditionally-initialized MM5 forecast over the same domains. As part of the same ATEC project MM5 forecasts are run twice daily (from 0600 and 1200 UTC) on the same grid configuration as the RT-FDDA system, but with traditional initializations from an analysis. The temperature statistics comparing the forecasts from the 1200 UTC traditional system and the forecasts in the RT-FDDA system are shown in Fig. 5. The improvement of the RT-FDDA system forecasts (true forecasts, not the assimilation stages) over the traditionally-initialized forecasts is apparent for both bias and MAE. The forecasts initialized from the RT-FDDA system have less error. The graphs of the statistics comparing the 0600 UTC traditional forecast to the RT-FDDA forecast are not shown because of space considerations but the differences are more

dramatic. It should be noted that there are some model configuration differences between the above systems. The traditional forecast system includes the MM5 land-surface model (LSM; Chen and Dudhia, 2000). The LSM is not implemented in the RT-FDDA system; the model configuration in curves A and D uses the simple climatology-based MM5 slab model. The model configuration in curves B and E uses a bucket soil moisture scheme and a simple snow fall/melt scheme (Low-Nam et al., 2001).

8. REFERENCES

- Charney, J.M., M. Halem, and R. Jastrow, 1969: Use of incomplete historical data to infer the present state of the atmosphere. *J. Atmos. Sci.*, 26, 1160-1163.
- Chen, F., and J. Dudhia, 2000: Coupling an advanced land-surface/hydrology model with the Penn State/NCAR MM5 modeling system. Part I: Model implementation and sensitivity. *Mon. Wea. Rev.*,
- Cram, J.M., J. Daniels, W. Bresky, Y. Liu, S. Low-Nam, R-S. Sheu, 2001: Use/impact of NESDIS GOES wind data within an operational mesoscale RT-FDDA system. *Preprints 18th WAF and 14th NWP Confs.*, Ft. Lauderdale, AMS. 5 pp.
- Fast, J.D., 1995. Mesoscale modeling and four-dimensional data assimilation in areas of highly complex terrain. *J. Appl. Meteor.*, 34, 2762-2782.
- Gray, D. J. Daniels, S. Nieman, S. Lord, and G. Dimego, 1996: NESDIS and NWS Assessment of GOES 8/9 Operational satellite motion vectors. *Proceedings 3rd Int. Winds Workshop*, Ascona, Switzerland. EUMETSAT Pub. EUM P18, ISSN 1023-0416, p175-183.
- Grell, G.A., J. Dudhia, and D.R. Stauffer, 1995: A description of the Fifth-generation Penn State/NCAR Mesoscale Model (MM5). NCAR/TN-398, NCAR, Boulder, CO. 122 pp.
- Horel, J., M. Splitt, B. White, 2000: Mesowest: Cooperative mesonets in the western United States. *Preprints 14th Symposium on Boundary Layer and Turbulence*, 7-11 August 2000, Aspen, CO. AMS, Boston, MA. 414-417.
- Low-Nam, S., C.A. Davis, J.M. Cram, Y. Liu, and R-S. Sheu, 2001: Use of a snow prediction scheme in a mesoscale real-time FDDA system. *Preprints 18th WAF and 14th NWP Confs.*, Ft. Lauderdale, AMS. 5 pp.
- Leslie, L.M., J.F. LeMarshall, R.P. Morrison, C. Spinoso, R.J. Purser, N. Pescod, R. Seecamp, 1998: Improved hurricane track forecasting from the continuous assimilation of high quality satellite wind data. *Mon. Wea. Rev.*, 126, 1248-57.
- Nieman, S.J., W.P. Menzel, C.M. Hayden, D. Gray, S. Wanzong, C. Velden, and J. Daniels, 1997: Fully automated cloud-drift winds in NESDIS operations. *Bull. Amer. Meteor. Soc.*, 78, 1121-1133.
- Seaman, N.L., D.R. Stauffer, A. M. Lario-Gibbs, 1995: A multiscale four-dimensional data assimilation system applied in the San Joaquin valley during SARMAP. Part I: Modeling design and basic performance characteristics. *J. Appl. Meteor.*, 34, 1739-1761.
- Stauffer, D.R., N.L. Seaman, and F.S. Binkowski, 1991: Use of four-dimensional data assimilation in a limited-area mesoscale model. Part II: Effects of data assimilation within the planetary boundary layer. *Mon. Wea. Rev.*, 119, 734-54.
- Stauffer, D.R., and N.L. Seaman, 1994: Multiscale four-dimensional data assimilation. *J. Appl. Meteor.*, 33, 416-434.